

# Tetranuclear Complexes Based on a Dynamic Metal–Metal Linkage, $[(\mu_4\text{-X})\text{Rh}_4(\text{CO})_4(\text{PNNP})_2]^{n+}$ ( $\text{X}/n = \text{RC}\equiv\text{C}/1$ (Acetylide), $\text{C}_2/0$ (Dicarbide))

Shukichi Tanaka, Christian Dubs, Akiko Inagaki, and Munetaka Akita\*

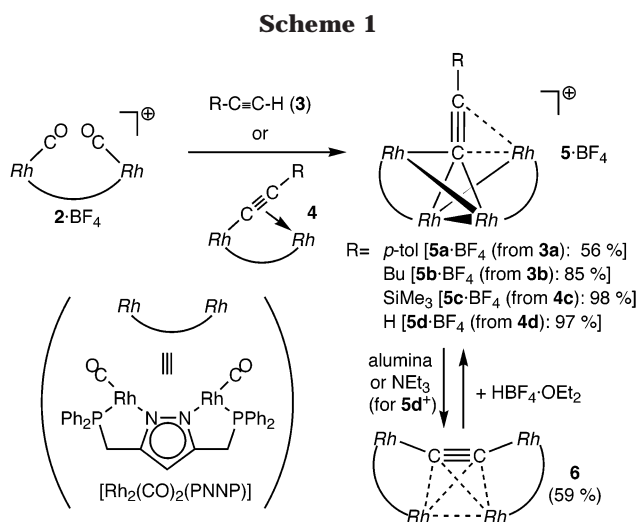
Chemical Resources Laboratory, Tokyo Institute of Technology, 4259 Nagatsuta, Midori-ku, Yokohama 226-8503, Japan

Received November 23, 2003

**Summary:** Tetra-rhodium complexes with a PNNP auxiliary,  $[(\mu_4\text{-X})\text{Rh}_4(\text{CO})_4(\text{PNNP})_2]^{n+}$  ( $\text{X}/n = \text{RC}\equiv\text{C}/1$  (acetylide),  $\text{C}_2/0$  (dicarbide); PNNP = 3,5-bis((diphenylphosphino)methyl)pyrazolato), are integrated mainly through M–X interactions and exhibit unique dynamic behavior associated with reversible metal–metal bond cleavage and recombination processes.

The chemistry of transition-metal cluster compounds constitutes a substantial part of organometallic chemistry, and previous studies have revealed a variety of structural motifs not only for the coordination mode of the organyl moiety but also for the metal framework.<sup>1</sup> Metal–metal bonds have been regarded as the major structural motif for the metal framework. However, little attention has been paid to polynuclear organometallic systems, which are not supported by metal–metal bonds, in contrast to relevant inorganic systems such as polyoxometalates. We have been studying polynuclear complexes containing a PNNP ligand (PNNP = 3,5-bis((diphenylphosphino)methyl)pyrazolato).<sup>2</sup> This PNNP ligand has the feature that the two metal centers bridged by it are at a distance longer than the M–M bonding interaction and, therefore, a metal–metal bond cannot be formed between them. In a previous paper<sup>3</sup> we reported the tetranuclear  $\mu_4$ -hydride complex  $[(\mu_4\text{-H})\text{Rh}_4(\text{CO})_4(\text{PNNP})_2]^+$  (**1**<sup>+</sup>), in which the four metal centers are bound together only through H–Rh interactions. Herein we wish to report the unique tetranuclear complexes, which turn out to be dynamic with respect to cleavage and recombination of metal–metal bonds.

Reaction of the labile cationic dinuclear tetracarbonyl complex  $[\text{Rh}_2(\text{CO})_4(\text{PNNP})]\text{BF}_4$  (**2**·BF<sub>4</sub>) with 1-alkyne (**3**; R = *p*-tol, Bu)<sup>4</sup> or the dinuclear  $\mu$ -acetylide complex  $[(\mu\text{-}\eta^1\text{-}\eta^2\text{-RC}\equiv\text{C})\text{Rh}_2(\text{CO})_2(\text{PNNP})]$  (**4**; R = SiMe<sub>3</sub>, H),<sup>5</sup> yielded the deep purple-red products **5**·BF<sub>4</sub> in good yields (Scheme 1).<sup>6,7</sup> Although the ESI-MS spectra of **5**·BF<sub>4</sub> revealed the formation of cationic tetranuclear acetylide



complexes with the composition of  $[(\text{RC}\equiv\text{C})\text{Rh}_4(\text{CO})_4(\text{PNNP})_2]^+$  through a  $1/2 \text{RC}\equiv\text{C}/\text{Rh}_2(\text{PNNP})$  coupling, unique but complicated dynamic behavior was observed for them. For example, the *p*-tolylethynyl complex **5a**·BF<sub>4</sub><sup>6</sup> showed a single <sup>31</sup>P NMR resonance ( $\delta_{\text{P}}$  56.3) at 25 °C, which separated into two signals below –42 °C (Figure 1a). The two signals as well as the different P–Rh coupling constants (**5a**<sup>+</sup>: 195 Hz ( $\delta_{\text{P}}$  64.5); 171 Hz ( $\delta_{\text{P}}$  61.4)) revealed that **5a**<sup>+</sup> contained two types of rhodium atoms located in different environments. No further change was observed, even when the sample was cooled to –90 °C. The fact that the  $J_{\text{P-Rh}}$  value at 25 °C (183 Hz) is precisely the average of the  $J_{\text{P-Rh}}$  values observed at –90 °C ( $(195 + 171)/2 = 183$ ) confirms that the single  $\delta_{\text{P}}$  signal at 25 °C results from coalescence of the two signals observed at low temperatures. In accord with the change in the <sup>31</sup>P NMR spectrum, the acetylide  $\alpha$ -carbon signal, which was observed at 25 °C as a quintet of quintets due to coupling with the four equivalent RhP units (Figure 1b), changed into an irresolvable multiplet at low temperatures, whereas the  $\beta$ -carbon signal appeared as a broad signal irrespective of temperature, presumably due to a weaker interaction with the  $[\text{Rh}_2(\text{PNNP})]_2$  moiety compared with that of the  $\alpha$ -carbon atom. The lack of <sup>1</sup>J<sub>C–H</sub> coupling for the  $\alpha$ -carbon signal clearly indicated formation of an acetylide cluster compound resulting from deprotonation of the  $\equiv\text{CH}$  moiety (from **3**).<sup>8</sup> Similar spectroscopic features were noted for the other complexes.<sup>6</sup> These spectroscopic features suggest that (1) the Rh<sub>4</sub> metal framework is unsymmetrical with respect to the

(1) Abel, E. W.; Stone, F. G. A.; Wilkinson, G. *Comprehensive Organometallic Chemistry II*; Pergamon: Oxford, U.K., 1995; Vols. 3–10. Dyson, P. J.; McIndoe, J. S. *Transition Metal Carbonyl Cluster Chemistry*; Gordon and Breach Science: Amsterdam, 2000. Shriver, D. F.; Kaesz, H. D.; Adams, R. D. *The Chemistry of Metal Cluster Complexes*; VCH: New York, 1990.

(2) Schenk, T. G.; Downs, J. M.; Milne, C. R. C.; Mackenzie, P. B.; Boucher, H.; Whelan, J.; Bosnich, B. *Inorg. Chem.* **1985**, *24*, 2334. Schenk, T. G.; Milne, C. R. C.; Sawyer, J. F.; Bosnich, B. *Inorg. Chem.* **1985**, *24*, 2338. See also: Bosnich, B. *Inorg. Chem.* **1999**, *38*, 2554.

(3) Tanaka, S.; Akita, M. *Angew. Chem., Int. Ed.* **2001**, *40*, 2865.

(4) Complexes **5a, b**<sup>+</sup> were also obtained from **2**<sup>+</sup> and the dinuclear acetylide complexes **4a, b**, respectively.

(5) Complexes **4** were prepared by treatment of **2**·BF<sub>4</sub> with LiC≡CR. Tanaka, S.; Inagaki, A.; Akita, M. To be submitted for publication.

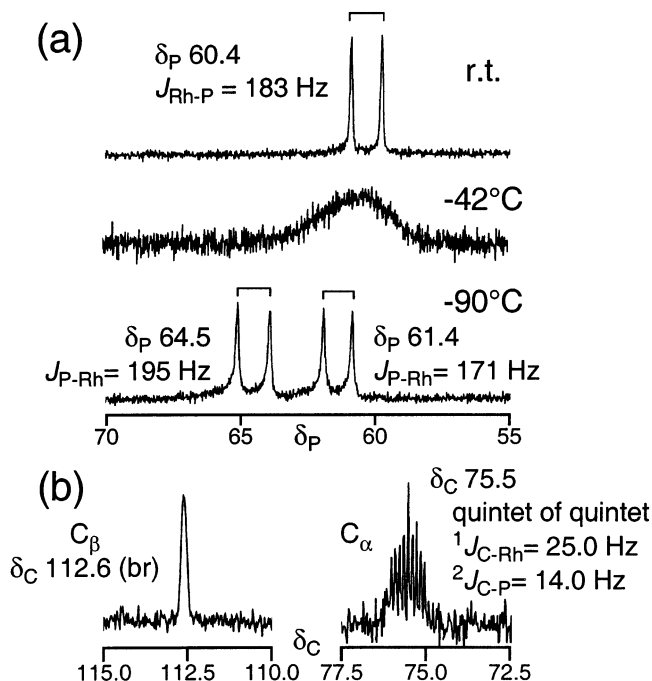


**Figure 1.** NMR spectra for **5a**·BF<sub>4</sub> observed in CD<sub>2</sub>Cl<sub>2</sub>: (a) variable-temperature <sup>31</sup>P NMR spectra observed at 81 MHz; (b) <sup>13</sup>C NMR spectra for the C≡C part observed at 25 °C at 100 MHz.

RC≡C moiety but exhibits dynamic behavior that averages all Rh coordination environments at higher temperatures and (2) the  $\alpha$ - and  $\beta$ -carbon atoms of the acetylide part are  $\sigma$ - and  $\pi$ -bonded to the Rh<sub>4</sub> framework, respectively: i.e.,  $\mu_4\text{-}\eta^1(\text{C}_\alpha)$  and  $\eta^2(\text{C}_\alpha\equiv\text{C}_\beta)$  coordination.

The molecular structure of the *p*-tolylethynyl complex **5a**·BPh<sub>4</sub> was determined by X-ray crystallography (Figure 2a).<sup>10</sup> Although the four rhodium atoms are arranged in a butterfly-like array,<sup>1</sup> it should be noted that the two Rh···Rh distances (Rh1···Rh2 = 3.6767(4) Å; Rh3···Rh4 = 3.7592(6) Å)<sup>9</sup> exceed the range of the bonding interaction in contrast to the other Rh–Rh distances of ca. 2.9 Å. The metal array observed for **5a**<sup>+</sup>

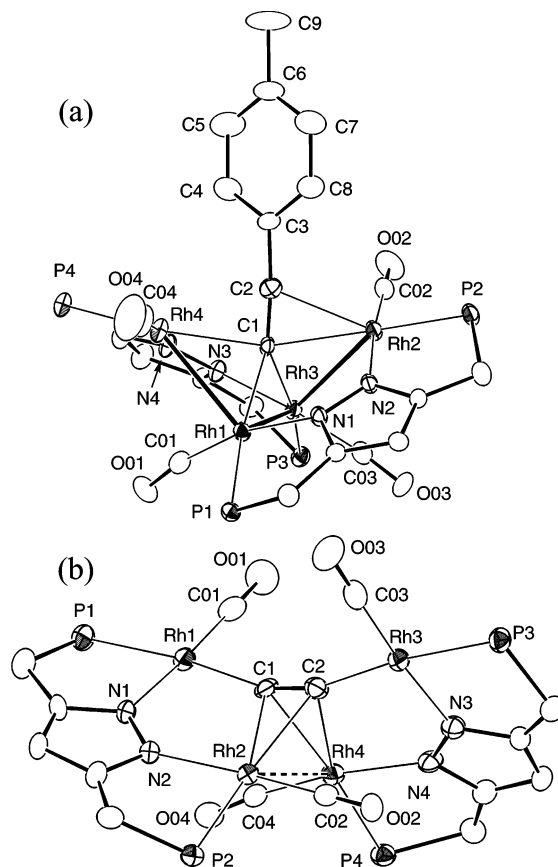


**Figure 2.** ORTEP views for (a) the cationic part of **5a**·BPh<sub>4</sub> and (b) **6**. Phenyl groups are omitted for clarity. Selected bond distances (in Å) and bond angles (in deg) are as follows. **5a**·BPh<sub>4</sub>: Rh1–Rh3 = 2.8925(4), Rh1–Rh4 = 2.9474(5), Rh2–Rh3 = 2.9732(5), C1–C2 = 1.249(7), C1–Rh1 = 2.151(4), C1–Rh2 = 2.309(4), C1–Rh3 = 2.223(4), C1–Rh4 = 2.335(4), C2–Rh2 = 2.386(5), C2···Rh4 = 2.555(5); Rh3–Rh1–Rh4 = 80.13(2), Rh1–Rh3–Rh2 = 77.62(1), C1–C2–C3 = 172.3(5). **6**: C1–C2 = 1.22(1), C1–Rh1 = 2.04(1), C1–Rh2 = 2.438(8), C1–Rh4 = 2.396(7), C2–Rh2 = 2.408(7), C2–Rh3 = 2.06(1), C2–Rh4 = 2.441(8), Rh1···Rh2 = 3.815(1), Rh1···Rh4 = 3.762(1), Rh2···Rh3 = 3.7826(8), Rh2–Rh4 = 3.1727(9), Rh3···Rh4 = 3.849(1); Rh1–C1–C2 = 163.4(7), Rh3–C2–C1 = 164.0(7), Rh1–C1–Rh2 = 116.5(3), Rh3–C2–Rh4 = 117.2(4), C1–Rh2–C2 = 29.2(3), C1–Rh4–C2 = 29.2(3).

(6) For experimental details, see the Supporting Information.

(7) We also attempted synthesis of the Ir<sub>4</sub> and Rh<sub>2</sub>Ir<sub>2</sub> derivatives. They were detected by ESI-MS and <sup>31</sup>P NMR but could not be isolated, owing to their lability.

(8) The formation of **5**<sup>+</sup> from **2** and **3** should proceed by way of the dinuclear intermediate **4**.<sup>4</sup> The viability of a deprotonation process in the formation of **5** from 1-alkyne (**3**) is supported by the observation that the reaction was promoted by a basic solvent; i.e., the reaction in acetone was faster and cleaner than that in CH<sub>2</sub>Cl<sub>2</sub>.

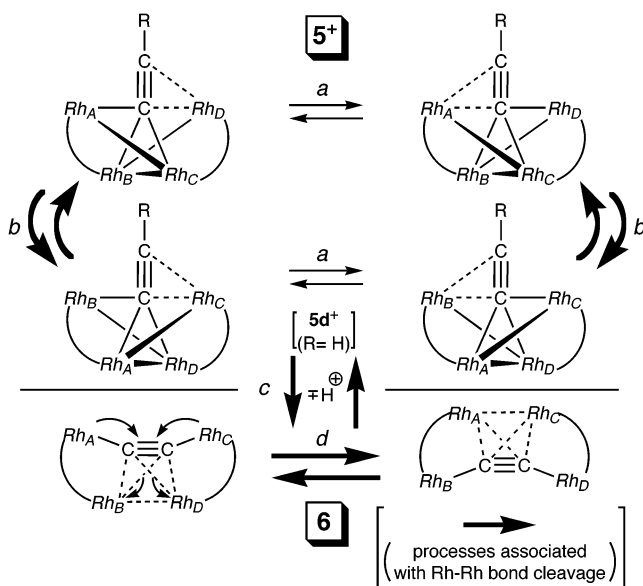
(9) Except for the unusually long Rh–Rh separation observed for a dodecarhodium cluster compound (3.567 Å),<sup>9a</sup> Rh–Rh distances are shorter than 3.3 Å. For example, the longest Rh–Rh distance in dinuclear complexes cited in the CSD is found for [Rh<sub>2</sub>(CN–C<sub>6</sub>H<sub>4</sub>–*p*-F)<sub>8</sub>]<sup>2+</sup> (3.293 Å).<sup>9b</sup> (a) Albano, V. G.; Chini, P.; Martinengo, S.; Sansoni, M.; Strumolo, D. *J. Chem. Soc., Dalton Trans.* **1978**, 459. (b) Endres, H.; Gottstein, N.; Keller, H. J.; Martin, R.; Rodemer, W.; Steiger, W. *Z. Naturforsch., B* **1979**, *34*, 827.

(10) X-ray diffraction measurements were made on a Rigaku RAXIS IV imaging plate area detector with graphite-monochromated Mo K $\alpha$  radiation at –60 °C. Crystal data for **5a**·BPh<sub>4</sub>: C<sub>95</sub>H<sub>77</sub>BN<sub>4</sub>O<sub>4</sub>P<sub>4</sub>Rh<sub>4</sub>, fw 1884.94, monoclinic, space group *P2*<sub>1</sub>/*a*, *a* = 17.9746(3) Å, *b* = 27.7046(6) Å, *c* = 16.6001(3) Å,  $\beta$  = 90.8460(10)°, *V* = 8265.6(3) Å<sup>3</sup>, *Z* = 4, *d*<sub>calcd</sub> = 1.515 g cm<sup>–3</sup>,  $\mu$  = 0.917 mm<sup>–1</sup>, R1 (wR2) = 0.043 (0.127) for the 11 068 unique data with *I* > 2 $\sigma$ (*I*) and 1010 parameters. Crystal data for **6**: C<sub>64</sub>H<sub>50</sub>N<sub>4</sub>O<sub>4</sub>P<sub>4</sub>Rh<sub>4</sub>, fw 1474.64, monoclinic, space group *P2*<sub>1</sub>/*c*, *a* = 22.608(3) Å, *b* = 19.320(3) Å, *c* = 14.927(4) Å,  $\beta$  = 110.979(4)°, *V* = 6087(1) Å<sup>3</sup>, *Z* = 4, *d*<sub>calcd</sub> = 1.609 g cm<sup>–3</sup>,  $\mu$  = 1.218 mm<sup>–1</sup>, R1 (wR2) = 0.068 (0.193) for the 8137 unique data with *I* > 2 $\sigma$ (*I*) and 721 parameters. CCDC: 218771 (**5a**·BPh<sub>4</sub>) and 218772 (**6**).

is best described as a folded Z-shaped linkage. As is suggested by the spectroscopic data, the  $\alpha$ -carbon atom of the acetylide ligand forms  $\sigma$ -bonding interactions with all four Rh centers and the C≡C moiety is  $\pi$ -bonded to one of the wingtip metal atoms, leading to the  $\mu_4\text{-}\eta^1(\text{C}_\alpha)\text{:}\eta^2(\text{C}_\alpha\equiv\text{C}_\beta)$  coordination.

The temperature-dependent NMR behavior of **5**<sup>+</sup> described above has been interpreted in terms of a combination of flipping of the acetylide ligand (path a) and reorganization of the folded Z-shaped metal linkage (path b) (Scheme 2), although a spectrum at the slow exchange limit, which is consistent with **5**<sup>+</sup> with no element of symmetry, has not been obtained. The two processes can be regarded as modified versions of the well-documented windshield wiper motion of the acetylide ligand: between the wingtip metal atoms (path a) and between the intra-PNNP-unit wingtip–hinge metal atoms (path b). The subtle difference in the C2–Rh2 and C2–Rh4 distances (~0.17 Å) in **5a**·BPh<sub>4</sub> suggests

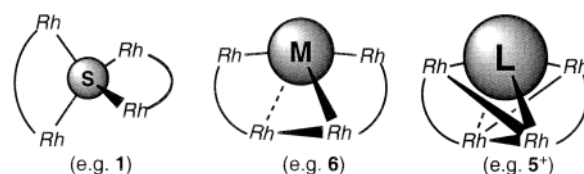
Scheme 2



that the lower energy process, which could not be frozen out even at  $-90\text{ }^{\circ}\text{C}$ , should be ascribed to the least-motion process (path a). It is notable that the higher energy process (path b) involves reversible cleavage and recombination of the metal–metal bonds.

The NMR data for the  $\equiv\text{CH}$  part of the ethynyl complex  $5\mathbf{d}\cdot\text{BF}_4$  ( $\delta_{\text{H}} 6.82$ ;  $J_{\text{C-H}} = 237\text{ Hz}$ ) suggests its acidic character. Accordingly, treatment of  $5\mathbf{d}\cdot\text{BF}_4$  with alumina or  $\text{NET}_3$  resulted in deprotonation to give the neutral  $\text{C}_2$  complex  $6$ ,<sup>11</sup> and the resultant product  $6$  reverted to  $5\mathbf{d}\cdot\text{BF}_4$  upon protonation with  $\text{HBF}_4\cdot\text{OEt}_2$  (Scheme 1). The simple NMR features for  $6$  (single  $\delta_{\text{C}}(\text{C}\equiv\text{C})$  and  $\delta_{\text{P}}$  signals), which did not change even when the sample was cooled as low as  $-90\text{ }^{\circ}\text{C}$ ,<sup>6</sup> suggested formation of a symmetrical structure, and the  $^{13}\text{C}$  NMR signal for the  $\text{C}_2$  bridge was located at  $\delta_{\text{C}} 98.9$  (multiplet). X-ray crystallography of  $6$ <sup>10</sup> (Figure 1b) revealed the tetranuclear  $\mu_4$ -dicarbide structure, in which the  $\text{C}_2$  bridge interacts with each  $\text{Rh}_2(\text{PNNP})$  fragment in a  $\mu\text{-}\eta^1\text{:}\eta^2$  fashion. The  $\text{C}\equiv\text{C}$  length is  $1.22\text{-}(1)\text{ \AA}$ , and the structure of the dinuclear moiety ( $\mu\text{-C}_2$ )- $[\text{Rh}_2(\text{PNNP})]$  is found to be similar to that of the dinuclear complex  $4$ .<sup>5</sup> Complex  $6$  is a rare example of such a type of compound ( $(\mu_4\text{-}\eta^1\text{:}\eta^1\text{:}\eta^2\text{:}\eta^2\text{-C}_2)\text{M}_4$ )<sup>13</sup> but, in comparison with the previous examples, the ( $\mu_4\text{-C}_2$ ) $\text{M}_4$  moiety is folded to a considerable extent. The dihedral angle between the  $\text{C}1\text{-C}2\text{-Rh}2$  plane and the  $\text{C}1\text{-C}2\text{-Rh}4$  plane is  $94.8^{\circ}$ , which is substantially more acute

Scheme 3



than the corresponding dihedral angle in  $[(\mu_4\text{-C}_2)\text{Cu}_4(\text{Ph}_2\text{-Ppzpy})_2]^{2+}$  ( $129.0^{\circ}$ ).<sup>13b</sup> In addition, because the  $\text{Rh}2\text{-Rh}4$  separation ( $3.1727(9)\text{ \AA}$ ) falls in the longer end of  $\text{Rh-Rh}$  bond lengths,<sup>9</sup> the folding should result from the bonding interaction between the  $\text{Rh}2$  and  $\text{Rh}4$  atoms.<sup>12</sup> The inconsistency between the virtually  $\text{C}_2$ -symmetrical solid-state structure with two different P environments and the single  $^{31}\text{P}$  NMR signal is due to dynamic behavior via oscillation of the  $\text{C}_2$  ligand, i.e., concurrent switching of the  $\eta^1$  and  $\eta^2$  coordination (d in Scheme 2),<sup>13c</sup> where the  $\sigma$ -bonded metal centers in one structure ( $\text{Rh}_{\text{A,C}}$ ) move to the  $\pi$ -bonded sites in the other structure. The activation barrier for the fluxional process should be very low, because the process was not frozen out even at  $-90\text{ }^{\circ}\text{C}$ . It is notable that (i) the fluxional behavior of  $6$  involves a  $\text{Rh-Rh}$  bond cleavage process and (ii) the deprotonation of  $5\mathbf{d}^+$  causes metal–metal bond cleavage to form  $6$ , protonation of which regenerates  $\text{M-M}$  bonds to give  $5\mathbf{d}^+$  (Scheme 1).

In summary, we have presented the synthesis and unique properties of the dynamic tetrahedral complexes  $[(\mu_4\text{-X})\text{Rh}_4(\text{CO})_4(\text{PNNP})_2]^{n+}$  ( $5^+$  and  $6$ ; Scheme 2). The fluxional processes involve reversible cleavage and recombination of the  $\text{Rh-Rh}$  bonds (paths b and d), and the  $\text{Rh}_4$  species  $5\mathbf{d}^+$  and  $6$  are interconverted with each other via the protonation–deprotonation cycle associated with cleavage of the  $\text{Rh-Rh}$  interaction (path c). The structure of the metal framework is dependent on the size of the bridging ligand (Scheme 3); i.e., a bulkier substrate should cause deformation of the symmetrical structure to bring metal atoms closer and form metal–metal bonds, and thus it was concluded that the polynuclear structures are integrated mainly through the  $\text{M-X}$  interactions rather than the  $\text{M-M}$  interactions. As a result, the metal–metal bonds become dynamic. Although non- $\text{M-M}$ -bonded polynuclear structures are known for group 11 metal species,<sup>1</sup> examples of other group metal complexes are still rare<sup>1</sup> and dynamic behavior via a reversible  $\text{M-M}$  cleavage process has few precedents.<sup>14</sup> Further studies using related ligand systems are now in progress.

**Acknowledgment.** This work was supported by a Grant-in-Aid for Scientific Research on Priority Areas (No. 15036222, “Reaction Control of Dynamic Complexes”) from the Ministry of Education, Culture, Sports, Science and Technology of Japan.

**Supporting Information Available:** Text and tables giving experimental and crystallographic details; crystallographic data are also available as CIF files. This material is available free of charge via the Internet at <http://pubs.acs.org>.

OM034315+

(11) Akita, M.; Moro-oka, Y. *Bull. Chem. Soc. Jpn.* **1995**, *68*.

(12) It is not always easy to determine the presence of a  $\text{M-M}$  bond only on the basis of the  $\text{M-M}$  distance. The maximum  $\text{Rh-Rh}$  bond length is  $3.3\text{ \AA}$ ,<sup>9</sup> whereas the covalent radius of  $\text{Rh}$  is  $1.25\text{ \AA}$ .<sup>12a</sup> In the case of  $6$ , the  $\text{Rh}2\text{-Rh}4$  bonding interaction ( $3.1727(9)\text{ \AA}$ ) should cause weak  $\text{Rh}2\cdots\text{C}04$  and  $\text{Rh}4\cdots\text{C}02$  interactions, leading to the slightly bent structure of the  $\text{Rh}2\text{-C}02\text{-O}02$  ( $173.4(7)^{\circ}$ ) and  $\text{Rh}4\text{-C}04\text{-O}04$  moieties ( $172.4(7)^{\circ}$ ) (cf.  $\text{Rh}1\text{-C}01\text{-O}01 = 179(1)^{\circ}$  and  $\text{Rh}3\text{-C}03\text{-O}03 = 179(1)^{\circ}$ ). The steric repulsion among the  $\text{CO}$  ligands, which project in the same direction as the  $\mu\text{-C}_2$  ligand does, may arrange the two rhodium centers close enough for bonding interaction leading to the folded structure. Emsley, J. *Elements*, 2nd ed.; Oxford University Press: Oxford, U.K., 1998.

(13) (a) Bruce, M. I.; Snow, M. R.; Tiekink, E. R. T.; Williams, M. L. *J. Chem. Soc., Chem. Commun.* **1986**, 702. (b) Song, H.-B.; Wang, Q.-M.; Zhang, Z.-Z.; Mak, T. C. W. *Chem. Commun.* **2001**, 1658. (c) Lo, W.-Y.; Lam, C.-H.; Fung, W. K.-M.; Sun, H.-Z.; Yam, V. W.-W.; Bacells, D.; Maseras, F.; Eisenstein, O. *Chem. Commun.* **2003**, 1260.

(14) See, for example: Akita, M.; Terada, M.; Moro-oka, Y. *Organometallics* **1992**, *11*, 1825 and references therein.